POLITECNICO DI TORINO
Repository ISTITUZIONALE

SoCNNet: An Optimized Sobel Filter Based Convolutional Neural Network for SEM Images Classification of Nanomaterials

Original
SoCNNet: An Optimized Sobel Filter Based Convolutional Neural Network for SEM Images Classification of Nanomaterials / Ieracitano, C., Paviglianiti, A., Mammone, N., Versaci, M., Pasero, E., Carlo Morabito, F. - In: Progresses in Artificial Intelligence and Neural Systems / Anna Esposito, Marcos Faundez-Zanuy, Francesco Carlo Morabito, Eros Pasero. - ELETTRONICO. - [s.l] : Springer, 2021. - ISBN 978-981-15-5093-5. - pp. 103-113 [10.1007/978-981-15-5093-5_10]

Availability:
This version is available at: 11583/2849884 since: 2020-12-10T14:23:59Z

Publisher:
Springer

Published
DOI:10.1007/978-981-15-5093-5_10

Terms of use:

This article is made available under terms and conditions as specified in the corresponding bibliographic description in the repository

Publisher copyright
Springer postprint/Author's Accepted Manuscript

This version of the article has been accepted for publication, after peer review (when applicable) and is subject to Springer Nature's AM terms of use, but is not the Version of Record and does not reflect post-acceptance improvements, or any corrections. The Version of Record is available online at: http://dx.doi.org/10.1007/978-981-15-5093-5_10

(Article begins on next page)

09 November 2026

SoCNNet: An Optimized Sobel Filter based Convolutional Neural Network for SEM images Classification of Nanomaterials

Cosimo Ieracitano[1,*], Annunziata Paviglianiti[2], Nadia Mammone[3], Mario Versaci[1], Eros Pasero[2], and Francesco Carlo Morabito[1]

[1] DICEAM Department, University Mediterranea of Reggio Calabria, 89124 Reggio Calabria, Italy
[2] Department of Electronic Engineering, Polytechnic of Turin, C.so Duca Degli Abruzzi 24, 10137 Turin, Italy
[3] IRCCS Centro Neurolesi Bonino-Pulejo, Via Palermo c/da Casazza, SS. 113 98124, Messina, Italy
[*] email:cosimo.ieracitano@unirc.it

Abstract. In this paper an optimized deep Convolutional Neural Network (CNN) for the automatic classification of Scanning Electron Microscope (SEM) images of homogeneous (HNF) and nonhomogeneous nanofibers (NHNF) produced by electrospinnig process is presented. Specifically, SEM images are used as input of a Deep Learning (DL) framework consisting of: a Sobel filter based pre-processing stage followed by a CNN classifier. Here, such DL architecture is denoted as *SoCNNet*. The Polyvinylacetate (PVAc) SEM image of NHNF and HNF dataset collected at the *Materials for Environmental and Energy Sustainability Laboratory* of the University Mediterranea of Reggio Calabria (Italy) is used to evaluate the performance of the developed system. Experimental results (average accuracy rate up to 80.27%±0.0048) demonstrate the potential effectiveness of the proposed SoCNNet in the industrial chain of nanofibers production.

Keywords: Nanofibers, Sobel, Laplacian, Fuzzy, Convolutional Neural Network

1 Introduction

Nanofibers (NF) produced by electrospinning process have gained a great deal of interest due to their unique mechanical properties and the wide range of potential real-world applications, including electronics [1], medicine [2], tissue engineering [3], drug delivery [4] and so on. NF are very thin fibers and exhibit diameters less then 100 nm. However, the fabrication of NF is very difficult to control. Indeed, electrospun fibers may be affected by manufactoring faults due to the instability of the polymeric jet attributable to undesirable processing parameters such viscosity, surface tension or applied voltage [5] [6]. The result is an array of nonhomogeneous nanofibers (NHNF) where the most common problem

is the presence of *beads*. Notably, beads are micro/nano aggregates that alter the morphology and properties of the material, observed especially with low values of polymeric concentration. One of the most effective method to monitor the quality and morphology of electrospun fibers is to examine Scanning Electron Microscope (SEM) images obtained from the NF sample under analysis. However, visual examination of SEM images is time consuming and is not the most efficient practice to detect and analyze potential defects in NF. In this context, intelligent systems able to discriminate automatically SEM images of homogeneous nanofibers (HNF, anomalies-free) and NHNF via advanced machine learning techniques (i.e. *deep learning*, DL [7]) have been emerging. DL has been successfully employed in several applications ([8], [9], [10]) but only a few works on anamaly detection in NF are reported in the literature. In [11], Carrera et al. developed an one-class classification approach based on a dictionary of patches of HNF proposed in [12]. The dictionary was applied to detect defects in a patch-wise fashion, reporting very good performance in identifying also small defects. In a second work [13], the authors implemented a CNN based system for detecting and localizing defects in SEM images. Anomaly patches were identified via similarity among test-patches under analysis and HNF patch of the dictionary. Recently, Ieracitano et al. [14] proposed a DL based anamoly detection system for classifying NHNF and HNF of PVAc nanfibers. The authors developed a deep CNN and used raw SEM images as input of the proposed network, reporting accuracy rate up to 80%. However, no data-preprocessing or validation techniques were applied. In contrast, here, motivated by the promising results achieved in [14], we propose an optimized DL system for discriminating SEM images of NHNF and HNF. Specifically, the proposed DL framework consists of three main modules: *electrospinning process, SEM image pre-processing, SEM-image classification*. Electrospinning process module includes electrospun NF production and NHNF/HNF SEM images collection [14]. SEM image pre-processing module includes the application of three different set of filters (i.e. Sobel, Laplacian, Fuzzy) in order to detect only the edge of each image and consequently make the classification task easier. In the SEM-image classification module, instead, pre-processed SEM images are used as input of the deep CNN for performing the NHNF vs HNF classification task. Experimental results showed that the Sobel filtering was able to improve the CNN discrimination performance (accuracy of 80.27% $\pm$ 0.0048, Table 1). Here, such optimized DL based anomaly detection system (consisting of Sobel + CNN) is denoted as *SoCNNet* (Figure 4).

The rest of this work is organized as follows. Section 2 introduces the proposed method, including the electrospinning process, SEM-image pre-processing and CNN based SEM-image classification. Section 3 reports the achieved results. Section 4 concludes the paper.

2 Methodology

Figure 1 reports the proposed framework. It includes three main processing units:

1. *Electrospinnig process*. PVAc nanofibers are produced through electrospinning process by dissolving PVAC in Ethanol (EtOH) solvent and SEM images of HNF and NHNF are stored on a computer according to the procedure described in [14].
2. *SEM image pre-processing*. Each HNF/NHNF SEM image is pre-processed by using Sobel, Laplacian and Fuzzy filtering, capable of providing information on the object contours of an image under analysis.
3. *SEM image classification*. Pre-processed SEM images are used as input of a CNN based classifier able to discriminate HNF and NHNF images automatically.

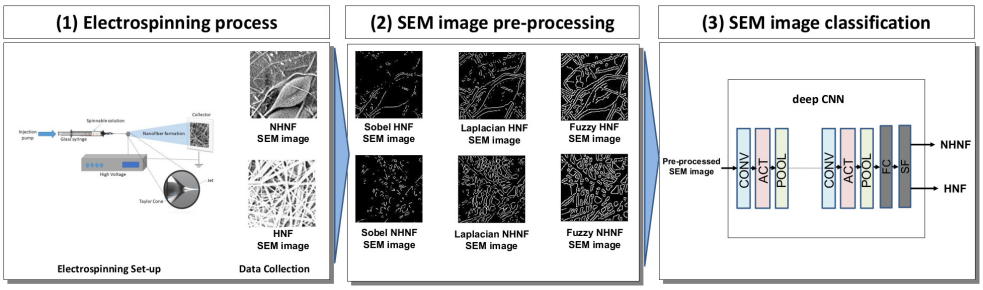

Fig. 1. Procedure of the proposed method.

2.1 Electrospinning Process

The basic set-up of the electrospinning (ES) process is schematically shown in Figure 2. It consists of a high voltage generator, a syringe pump and a grounded collector plane. Firstly, the polymer fluid is introduced into a glass syringe and extruded through the spinneret by external pumping (at a constant and controllable flow rate) until a small droplet is formed. Then, a high voltage is applied between the collecting (i.e. collector surface, cathode) and spinning (i.e. needle, anode) electrode. As the electric field increases, the droplet deforms into a conical shape, known as *Taylor cone* [15]. Specifically, when the electrostatic repulsion is greater than the surface tension of the droplet, a charged jet is ejected from the tip of the cone towards the collector plane. During the jet emission, the solvent evaporates and the solidified fibers are collected on the target.

It has been proven that viscosity and concentration of the polymeric solution mainly affect the diameter and morphology of nanofibers. For example, low values of concentration cause the production of micro-particles (i.e. *beads*) due to the electrospray phenomenon [16]. Other important electrospinning parameters are applied voltage, tip-collector distance and flow-rate [17].

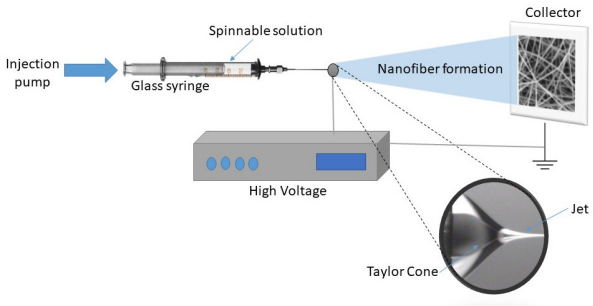

Fig. 2. Set-up of the electrospinning process.

Materials. Here, Polyvinylacetate (PVAc) with average molecular weight (M_w) of 170 * 10^3 g/mol and Ethanol (EtOH) are employed as polymer and solvent, respectively. Specifically, PVAc is dissolved in EtOH solvent by using a magnetic stirrer until a clear fluid is achieved. The CH-01 Electrospinner 2.0 (Linari Engineering s.r.l.) with a 20 mL glass syringe with a stainless steel needle of 40 mm length and 0.8 mm thick is used for the nanofiber production. Moreover, it is to be noted that the spinning process is carried out at a temperature and air humidity of 20±1 C and 40% respectively. The morphology of the produced PVAc nanofiber is analyzed through the Phenom Pro-X scanning electron microscope (SEM) that included an energy-dispersive x-ray spectrometer. Then, the Fibermetric software is used in order to evaluate the average diameter of the electrospun fiber and detect the potential presence of defects (i.e. beads). The experiments included 16 different setup, where concentration (e_1), voltage e_2, flow rate e_3 and tip-collector distance e_4 parameter were changed one at time in well-known working conditions: 10-25 wt.% e_1; 10-17.5 kV e_2; 100-300 μL/min e_3; 10-15 cm e_4. Further details of the ES experiments can be found in [14].

Dataset Description. The SEM images dataset proposed in [14] was used. Specifically, it consists of 160 SEM images labeled by an expert as image of homogeneous nanofibers (HNF) or nonhomogeneous nanofibers (NHNF). Notably, the dataset includes 75 HNF and 85 NHNF sized 128 x 128 [14]. It is worth mentioning that the production HNF is typically observed with high values of voltages and concentrations; whereas, NHNF are affected by the presence of micro or nano structural anomalies (i.e. beads) that can occur when the polymeric solution is made up of low values of concetrations or when the TCD is too high. As an example, Figure 3 reports a NHNF and HNF SEM image of PVAc electrospun nanofiber.

2.2 SEM image pre-processing

In order to make the classification task easier for the proposed classier (Section 2.3), each NHNF/HNF SEM image $I(x, y)$, has been pre-processed by reducing

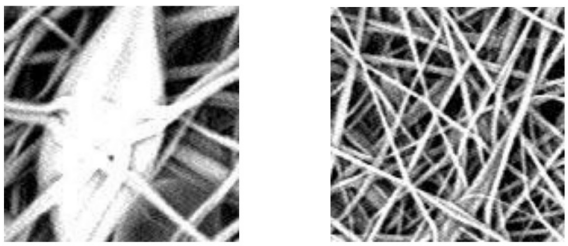

Fig. 3. (a) SEM image of nonhomogeneous nanofibers (NHNF) due to *beads*. (b) SEM image of homogeneous nanofibers (HNF).

the number of gray-scale levels but, simultaneously, maintaining the texture of the individual image as much as possible [18]. With this goal in mind, edge detection techniques are excellent candidates as they segment images based on information on the edges providing information on the object contours using some edge-detection operators finding discontinuity in the gray levels, color, texture, etc. the edge pixel (x, y) are pixel in which the intensity of brightness, $f(x, y)$, of the image changes abrutly and the edges (or segments of edge) are sets of connected pixels. By means of Sobel technique [18], edge detection is achieved by of a differential operator consisting of two convolution matrices 3×3 with integer values, $G_x = [0\ 1\ 2;\ -1\ 0\ 1;\ -2\ -1\ 0]$ and $G_y = [-2\ -1\ 0;\ -1\ 0\ 1;\ 0\ 1\ 2]$, which convoluted with the image I calculate an approximate value of $\nabla f(x, y) = [f_x(x, y),\ f_y(x, y)] = [G_x * I,\ G_y * I]$ indentifying the direction of greater variation of $f(x, y)$, $\theta = tan^{-1}(f_y(x, y)/f_x(x, y))$, together with its speed in the same direction identified by its magnitude $|\nabla f(x, y)| = \sqrt{f_x(x, y)^2 + f_y(x, y)^2}$. According to Marr and Hildred, instead, edge detection can be implemented using the filter $\nabla^2 G$, with $G(x, y) = e^{-\frac{x^2+y^2}{2\sigma^2}}$ obtaining $\nabla^2 G = ((x^2 + y^2 - 2\sigma^2)/\sigma^4)e^{-\frac{x^2+y^2}{2\sigma^2}}$ which represents the LoG filter (Laplacian of the Gaussian) [18]. However, to reduce the computational complexity of LoG, usually a convolution matrix 5×5, such as [0 0 −1 0 0; 0 −1 −2 −1 0; −1 −2 16 −2 −1; 0 −1 −2 −1 0; 0 0 −1 0 0], is used that approximates $\nabla^2 G$. Fuzzy edge detection is an alternative approach to edge detection which considers the image to be fuzzy because, often, in most of the images the edge are not clearly defined, so that detection can becomes very difficult. In this paper, a modified Chaira and Ray approach [19] exploiting the fuzzy divergence between the image window and each of a set of 16 convolution matrices (3×3, whose elements belong to the set $\{0.3,\ 0.8\}$ to ensure good edge detection) which represent the edge profile of different types is presented. Specifically, after normalizing the image I, the center of each convolution matrix is place on each pixel (x, y) of I. Then, fuzzy divergence measure, $Div(x, y)$, between each of the elements of the image window and the template is calculed and the minimum value is selected. This procedure is repeated for

all of 16 convolution matrices selecting the maximum value among the 16 divergence values obtained. Then, we obtain a divergence matrix on which a threshold technique must be applied. For this purpose, in this paper a new entropic $2D$ fuzzy thresholding method based on minimization of fuzzy entropy is proposed. In particular, for each threshold T, set a square matrix W of size r centered on (x, y) and considered another window W' of the same dimensions centerd on another pixel (x', y'), their distance is first calculed by the fuzzy divergence [4]. The average value of all the fuzzy divergences obtained by moving (x', y') in all possible positions is then calculated. Moreover, we calculate the further average value obtained by moving (x, y) in all possible position. We indicate with $Mean_r$ the latter average value obtained. We repeat the procedure for square windows of size $r+1$, obtaining $Mean_{r+1}$. Then, Fuzzy Entropy depending on T, $FE(T)$ can be computed as $FE(T) = ln(Mean_r/Mean_{r+1})$ so that the optimum threshold, $T_{optimum}$ can be computed by means of $T_{optimum} = arg; min_T|FE(T)|$. Obviously, if necessary, a pre-treatment such as contrast enhancement could be implemented to improve the image quality globally [20], [21], [22].

2.3 SEM image classification

CNN Classifier Convolutional Neural Networks (CNN) is a DL technique capable of learning the most relevant features from the input representations through an architecture organized hierarchically. A standard CNN includes the following processing modules:

1. *convolutional layer (CONV)*: where, K_j filters (sized k_1 x k_2) convolve with the i^{th} input image I (sized h x w), producing j *features maps* (A) of size a_1 x a_2. Notably:

$$A_j = \sum I_i * K_j + B_j \tag{1}$$

where B_j represents the bias and * the convolution operation;

$$a_1 = \frac{h - k_1 + 2p}{s} + 1 \tag{2}$$

$$a_2 = \frac{w - k_2 + 2p}{s} + 1 \tag{3}$$

where s and p are the stride (or shift) and zero padding parameters, respectively. Specifically, the j^{th} filter convolves with a sub-region of the i^{th} input and shift over the whole input map with a stride s; whereas, p is typically used to control the output matrix dimension by padding the input edges with null values.

[4] Fuzzy divergence can be considered as a distance because it satisfies all the axioms of the metric spaces.

2. *activation layer (ACT)*: it includes a nonlinear transfer function. Specifically, '*Rectified Linear Unit*" (ReLu, $l(x) = max(0, x)$) activation function is typically used in CNN architecture (ACT_{ReLU}). Indeed, it achieves very good performance in terms of generalization and learning time [23].
3. *pooling layer (POOL)*: it reduces the input spatial size by evaluating the average (*average pooling,* $POOL_{avg}$) or maximum (*max pooling,* $POOL_{max}$) value of a sub-matrix conveniently selected by a filter sized $\tilde{f}_1$ x $\tilde{f}_2$. Here, the $POOL_{max}$ is employed. Notably, the filter slides over the input map with stride $\tilde{s}$ and takes the maximum of the sub-matrix under analysis. The results is a downsampled representation of A_j sized $\tilde{a}_1$ x $\tilde{a}_2$ with

$$\tilde{a}_1 = \frac{a_1 - \tilde{f}_1}{\tilde{s}} + 1 \tag{4}$$

and

$$\tilde{a}_2 = \frac{a_2 - \tilde{f}_2}{\tilde{s}} + 1 \tag{5}$$

The CNN typically ends with a standard fully connected (FC) neural network for classification purposes.

Here, the pre-processed (and raw) SEM images were used as input of the deep CNN previously proposed in [14]. Specifically, it included five modules of $CONV$+ACT_{ReLU}+$POOL_{max}$ and one fully connected layer (FC) with 40 hidden units followed by a softmax output layer to perform the NHNF vs. HNF classification task. Each $CONV$ layer had filters size k_1 x k_2 = 3 x 3, whereas shift and padding valus of s=1 and p=1, respectively. Each $POOL_{max}$ layer had filters size $\tilde{f}_1$ x $\tilde{f}_2$= 2 x 2 and stride $\tilde{s}$=2. All the learning paramentes were set up by following the recommnedations reported in [24]. The network was initialized through a Gaussian distribution having mean 0 and standard deviation 0.01. Moreover, the stochastic gradient descent technique with momentum= 9 * 10^{-1}, weight decay= 10^{-4}, learning parameter= 10^{-2}, mini-batch=32, was used. Further details can be found in [14].

3 Results

The evaluation performances were quantified in terms of precision (PC), recall (RC), F-measure (FM) and accuracy (ACC):

$$PR = \frac{TP}{TP + FP} \tag{6}$$

$$RC = \frac{TP}{TP + FN} \tag{7}$$

$$FM = 2 * \frac{PR * RC}{PR + RC} \tag{8}$$

$$ACC = \frac{TP + TN}{TP + TN + FP + FN} \tag{9}$$

where TP are the true positives: number of NHNF SEM images properly classified as NHNF; TN are the true negatives: number of HNF SEM images properly classified as HNF; FP are the false positives: number of HNF SEM images erroneously classified as NHNF; FN are the false negatives: number of NHNF SEM images erroneously classified as HNF. Moreover, the k-fold cross validation procedure (with k=15) was used. Notably, train and test sets included 70% and 30% of images (in each fold), respectively. Thus, all the outcomes are reported as average value ± standard deviation. Table 1 reports the NHNF vs. HNF classification performance when the CNN receives as input: raw SEM images (RaCNNet), pre-processed SEM images with Sobel filter (SoCNNet), pre-processed SEM images with Laplacian filter (LaCNNet) and pre-processed SEM images with Fuzzy based filter (FuCNNet). As can be seen, the Sobel approach, SoCNNet (Figure 4), outperforms all the others, achieving accuracy rate up to 80.27% ± 0.048 and F-measure of 82.81% ± 0.046. To the best of our knowledge, this is the first work on SEM images classification of HNF and NHNF of PVAc electrospun nanofibers by using a Sobel filter as pre-processor of a CNN architecture. There are only a few works that used DL for the automatic anomalies detection of SEM images. Notably, for fair comparison, we compared the results here presented with a recent work [14], where the same CNN structure and dataset was employed, reporting a classification accuracy of 80%. However, in [14], raw SEM images were used as input and no validation technique was applied. In contrast, here, we observed that the performance decreased to 74.69% with raw SEM images (RaCNNet, Table 1) using the 15-fold cross validation technique and most important the Sobel approach allowed to improve the classification performance of about 6% (SoCNNet, Table 1).

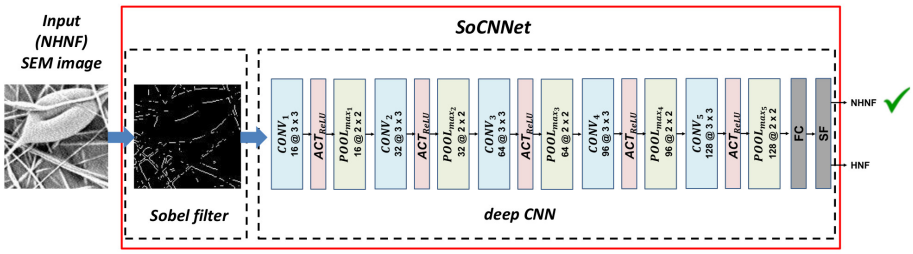

Fig. 4. SoCNNet: optimezed CNN, consisting of Sobel filer and the deep CNN proposed in [14].

4 Conclusion

In this research, we presented an optimized DL system for the automatic anomaly detection in SEM images of nanofibers produced by electrospinning process. Specifically, we improved the performance of the CNN architecture proposed

Table 1. Classification performance of the CNN when raw SEM images (RaCNNet), pre-processed SEM images with Sobel filter (SoCNNet), pre-processed SEM images with Laplacian filter (LaCNNet) and pre-processed SEM images with Fuzzy based filter (FuCNNet) are used as input. All the results are reported as average value ± standard deviation.

Method	Precision	Recall	F-measure	Accuracy
RaCNNet	$84.51\% \pm 7.7 \times 10^{-2}$	$71.46\% \pm 6.1 \times 10^{-2}$	$77.01\% \pm 3.3 \times 10^{-2}$	$74.69\% \pm 4.5 \times 10^{-2}$
SoCNNet	$83.62\% \pm 5.7 \times 10^{-2}$	$82.76\% \pm 8.7 \times 10^{-2}$	$82.81\% \pm 4.6 \times 10^{-2}$	$80.27\% \pm 4.8 \times 10^{-2}$
LaCNNet	$73.52\% \pm 7.6 \times 10^{-2}$	$68.00\% \pm 7.4 \times 10^{-2}$	$70.07\% \pm 3.5 \times 10^{-2}$	$66.54\% \pm 4.7 \times 10^{-2}$
FuCNNet	$74.20\% \pm 6.6 \times 10^{-2}$	$66.46\% \pm 9.5\times 10^{-2}$	$69.70\% \pm 6.5\times 10^{-2}$	$65.06\% \pm 6.6 \times 10^{-2}$

in [14], used to classify images of homogeneous (HNF) and nonhomogeneous nanofibers (NHNF), by pre-processing each SEM image through a Sobel based filter. Here, the combination of Sobel filtering and CNN was denoted as *SoCNNet*. In order to evaluate the effectiveness of the proposed model, the images were also pre-processed with other techniques (i.e. Laplacian and a Fuzzy based filters) and used as input of the deep CNN. Notably, the corresponding networks were denoted as LaCNNnet and FuCNNet, respectively. Furthermore, for fair comparison, raw SEM images were also the input of the CNN classifier (RaCNNet).Comparative results showed that the proposed SoCNNet (Figure 4) outperformed all the other systems LaCNNnet, FuCNNet and RaCNNet achieving accuracy rate up to $80.27\% \pm 0.048$. However, it is worth metioning that this is a preliminary study for a more accurate and versatile system. In the future, a more accurate investigation of the applied filters will be addressed. In addition, in order to estimate the feasibility of the proposed SoCNNet a lager image dataset produced by electrospinning process of PVAc and others polymers will be taken into account.

5 Acknowledgements

This work is supported by the project code: GR-2011-02351397. The authors would also like to thank the research group of the *Materials for Environmental and Energy Sustainability Laboratory* from the University Mediterranea of Reggio Calabria (Italy) from providing the SEM image dataset used in this work.

References

1. Wu, Y., Qu, J., Daoud, W.A., Wang, L., Qi, T.: Flexible composite-nanofiber based piezo-triboelectric nanogenerators for wearable electronics. Journal of Materials Chemistry A (2019)
2. Yang, Y., Chawla, A., Zhang, J., Esa, A., Jang, H.L., Khademhosseini, A.: Applications of nanotechnology for regenerative medicine; healing tissues at the nanoscale. In: Principles of Regenerative Medicine, pp. 485–504. Elsevier (2019)

3. Mo, X., Sun, B., Wu, T., Li, D.: Electrospun nanofibers for tissue engineering. In: Electrospinning: Nanofabrication and Applications, pp. 719–734. Elsevier (2019)
4. Topuz, F., Uyar, T.: Electrospinning of cyclodextrin functional nanofibers for drug delivery applications. Pharmaceutics 11(1), 6 (2019)
5. Entov, V., Shmaryan, L.: Numerical modeling of the capillary breakup of jets of polymeric liquids. Fluid dynamics 32(5), 696–703 (1997)
6. Yarin, A.L.: Free liquid jets and films: hydrodynamics and rheology. Longman Publishing Group (1993)
7. LeCun, Y., Bengio, Y., Hinton, G.: Deep learning. Nature 521(7553), 436–444 (2015)
8. Ieracitano, C., Adeel, A., Gogate, M., Dashtipour, K., Morabito, F.C., Larijani, H., Raza, A., Hussain, A.: Statistical analysis driven optimized deep learning system for intrusion detection. In: International Conference on Brain Inspired Cognitive Systems. pp. 759–769. Springer (2018)
9. Ieracitano, C., Mammone, N., Bramanti, A., Hussain, A., Morabito, F.C.: A convolutional neural network approach for classification of dementia stages based on 2d-spectral representation of eeg recordings. Neurocomputing 323, 96–107 (2019)
10. Dashtipour, K., Gogate, M., Adeel, A., Ieracitano, C., Larijani, H., Hussain, A.: Exploiting deep learning for persian sentiment analysis. In: International Conference on Brain Inspired Cognitive Systems. pp. 597–604. Springer (2018)
11. Carrera, D., Manganini, F., Boracchi, G., Lanzarone, E.: Defect detection in sem images of nanofibrous materials. IEEE Transactions on Industrial Informatics 13(2), 551–561 (2017)
12. Boracchi, G., Carrera, D., Wohlberg, B.: Novelty detection in images by sparse representations. In: Intelligent Embedded Systems (IES), 2014 IEEE Symposium on. pp. 47–54. IEEE (2014)
13. Napoletano, P., Piccoli, F., Schettini, R.: Anomaly detection in nanofibrous materials by cnn-based self-similarity. Sensors 18(1), 209 (2018)
14. Ieracitano, C., Panto, F., Mammone, N., Paviglianiti, A., Frontera, P., Morabito, F.C.: Towards an automatic classification of sem images of nanomaterial via a deep learning approach. In: Multidisciplinary Approaches to Neural Computing. *in press*
15. Doshi, J., Reneker, D.H.: Electrospinning process and applications of electrospun fibers. Journal of electrostatics 35(2-3), 151–160 (1995)
16. Fenn, J.B., Mann, M., Meng, C.K., Wong, S.F., Whitehouse, C.M.: Electrospray ionization for mass spectrometry of large biomolecules. Science 246(4926), 64–71 (1989)
17. Theron, S., Zussman, E., Yarin, A.: Experimental investigation of the governing parameters in the electrospinning of polymer solutions. Polymer 45(6), 2017–2030 (2004)
18. Gonzales, R., Woods, R.: Digital Image Processing. Pearson - Prentice Hall (2018)
19. Chaira, T., Ray, A.K.: Fuzzy image processing and applications with MATLAB. CRC Press (2009)
20. Versaci, M., Morabito, F.C., Angiulli, G.: Adaptive image contrast enhancement by computing distances into a 4-dimensional fuzzy unit hypercube. IEEE ACCESS 5, 26922–26931 (2017)
21. Versaci, M., Calcagno, S., Morabito, F.C.: Fuzzy geometrical approach based on unit hyper-cubes for image contrast enhancement. In: IEEE International Conference on Signal and Image Processing Applications (ICSIPA 2015). pp. 488–493. IEEE (2015)

22. Versaci, M., Calcagno, S., Morabito, F.C.: Image contrast enhancement by distances among points in fuzzy hyper-cubes. In: IEEE International Conference, CAIP 2015. pp. 494–505. IEEE (2015)
23. Nair, V., Hinton, G.E.: Rectified linear units improve restricted boltzmann machines. In: Proceedings of the 27th international conference on machine learning (ICML-10). pp. 807–814 (2010)
24. Bengio, Y.: Practical recommendations for gradient-based training of deep architectures. In: Neural networks: Tricks of the trade, pp. 437–478. Springer (2012)